A Versatile Trapped Ion Cell for Ion Cyclotron Resonance Spectroscopy

T. B. McMahon* and J. L. Beauchamp

Arthur Amos Noyes Laboratory of Chemical Physics,† California Institute of Technology, Pasadena, California 91109

(Received 4 October 1971; and in final form, 16 December 1971)

Experimental methods have been developed which permit operation of the standard ICR cell in a trapped ion mode. Appropriate configurations of applied electrostatic fields permit trapping of ions in the source region of the ICR cell. Detection is effected after a suitable delay by drifting the ions from the source through the analyzer region where their power absorption is monitored with the usual marginal oscillator–detector. The minor modifications required do not inhibit normal operation of the cell, thus allowing for the full range of conventional ICR experiments with the additional capability of examining variation of ion abundance with time. The latter mode of operation greatly simplifies elucidation of reaction kinetics. The ion molecule reactions of methyl chloride have been investigated using this new technique. Accepted values of reaction rate constants are reproduced, demonstrating the accuracy of the method.

INTRODUCTION

The technique of ion trapping in the negative space charge of an electron beam has been shown by Herod and Harrison[1] to be well suited to the determination of ion–molecule reaction rates in conventional mass spectrometers. Fluegge and Wobschall[2] have described a method for trapping ions for short periods of time (0–1.0 msec) in an ICR spectrometer and, more recently, McIver and co-workers have demonstrated that a trapped ion analyzer cell for ICR is a valuable tool for the determination of ion–molecule reaction rates.[3–6] The simple analysis required to relate reaction rate constants to the variation of ion abundance with time obviates the difficult task of calculating rate constants by iterative computer solution of the ICR power absorption equations.[7–9] This increased ease of calculation makes the variation of ion abundance with time far more amenable to the determination of reaction rate constants than the more usual study of the variation of ion abundance with pressure. However, the conventional cell remains well suited to routine study of numerous aspects of gas phase ion chemistry. These include examination of elastic collisions by collision broadening of the absorption line,[10,11] identification of reactions in double resonance experiments,[12] determination of product distributions using source[13,14] and trapping[15] ion ejection techniques, study of the variation of reaction rates with ion kinetic energy,[16,18] observation of collisional stabilization of excited intermediates in ion molecule reactions,[19,20] and the routine recording of mass spectra without mass discrimination.[11] While it is possible to perform many of these experiments using the trapped ion cell described by McIver and co-workers[3–6] it is our opinion that the conventional cell offers distinct advantages in most applications, primarily in terms of operational simplicity. Ideally, one would wish to be able to utilize the conventional ICR cell in ion trapping experiments. This paper describes appropriate modifications to the conventional ICR cell which provide this capability, allowing the examination of variation of ion abundance with reaction times up to 1 sec at a fixed pressure. The kinetic parameters obtained in this manner complement the information obtained from experiments in which the variation of ion abundance with pressure at a fixed reaction time is examined. It should be noted in the latter experiment that reaction time is, in fact, not fixed since it will depend on magnetic field strength which will be different for each mass ion. It is this complication that accounts to a large extent for the difficulty in obtaining kinetic data from studies of the variation of signal intensity with pressure.[7–9]

EXPERIMENTAL

The only physical alterations to the cell necessary to effect ion trapping are the addition of a plate to the rear of the source region (connected to either of the source drift plates) and the mounting of 90% open mesh grids between the filament and trapping plate on one side of the cell and between the electron collector and the trapping plate on the other. These grids, operated at the potential of the adjacent trapping plate, shield the trapping region of the cell from the bias voltages applied to the filament and electron collector and were found to greatly reduce ion losses during the trapping period. The standard ICR cell, modified for trapping experiments, is shown in Fig. 1. Included for comparison is the trapped ion cell described by McIver[3] which combines ion production and detection functions in the same region. The design features of both cells have been previously described.[3,21]

In a typical experiment ions are formed by an electron beam pulse of variable energy and duration. Trapping of positive ions is effected by keeping the source drift plates and the new rear plate at ground, the analyzer drift plates at some negative potential, and the trapping plates at a positive potential. This creates a potential configuration in the source very much like that in the trapped ion analyzer cell described by McIver. The space potential everywhere within the source is positive with respect to the surrounding electrodes and adjacent resonance region. This constrains the ions to move on equipotentials of the

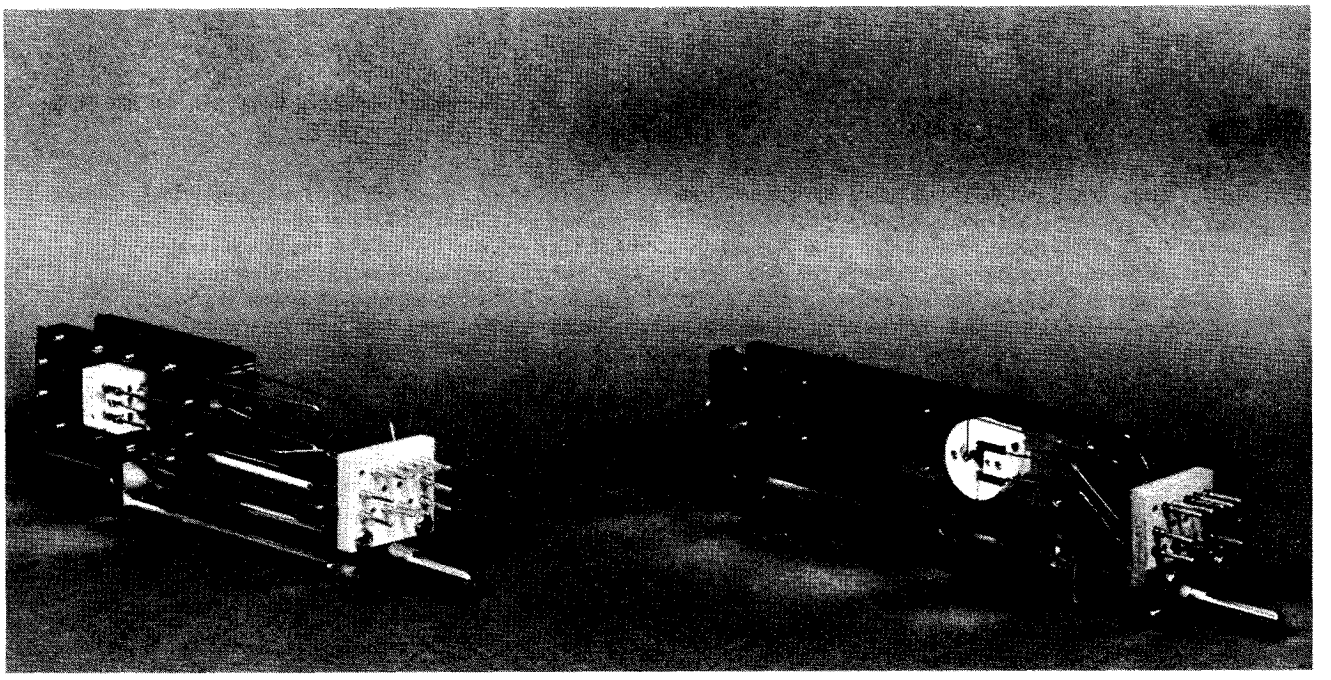

FIG. 1. Comparison of the McIver trapped ion analyzer cell (shown on left) with the conventional ICR flat cell modified for trapped ion mode of operation.

drift field which close on themselves within the source region of the cell.[22] To trap negative ions the polarity of the voltage applied to the trapping and analyzer drift plates is reversed.

Ion detection is effected by switching all voltages to appropriate values for the normal drift mode of operation as schematically illustrated in Fig. 2. The ions are thus drifted through the analyzer region of the cell where they are observed with a marginal oscillator detector. For experiments described in this paper, pulsing and timing sequences were provided by Tektronix 2600 series pulse units. Timing measurements were made with a Heath universal digital instruments model EU-805. The transient output at the marginal oscillator was *integrated* by a Princeton Applied Research model 160 boxcar integrator and the output displayed on an *xy* recorder. A schematic of the pulsing sequence used is illustrated in Fig. 3.

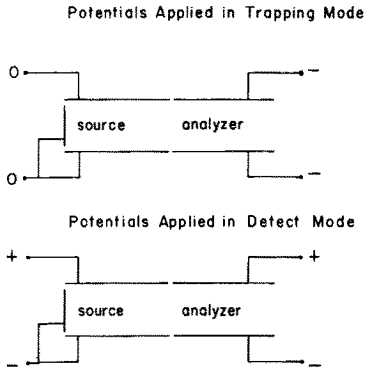

FIG. 2. Potentials applied to the trapped ion cell in trapping and detect modes.

DATA ANALYSIS AND APPLICATIONS

The instantaneous power absorption of ions at resonance is given by[7,23]

$$A(t)=\frac{N(0)q^2E_{\mathrm{rf}}{}^2t}{4m}, \tag{1}$$

where $N(0)$ is the number of ions with mass to charge ratio m/q, E_{rf} is the radio frequency electric field strength and t is the time the ions have been in the analyzer region. The drift velocity of ions in the resonance region is determined by the static electric field strength $\mathbf{E}$ and the magnetic field strength $\mathbf{H}$ according to the relation[24]

$$\mathbf{v}_D=\frac{c\mathbf{E}\times\mathbf{H}}{H^2}. \tag{2}$$

Thus, knowing the drift velocity from Eq. (2) and the length l of the resonance region the drift time through the resonance region is given by

$$\tau=lH/cE, \tag{3}$$

when $\mathbf{H}$ and $\mathbf{E}$ are perpendicular fields. Hence, the power absorption increases linearly with time, rising to a maximum at $t=\tau$, beyond which it falls to zero as the ions leave the resonance region. The boxcar detector utilized in the present experiments integrates the transient power absorption, giving the measured signal intensity

$$I=N(0)\frac{q^2E_{\mathrm{rf}}{}^2\tau^2}{8m}. \tag{4}$$

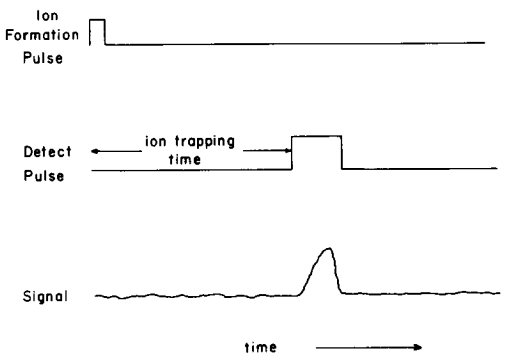

FIG. 3. Pulsing sequence used for trapped ion cell experiments. Typical pulse widths are 3 msec ion formation pulse and 5 msec detect pulse. The detect pulse simultaneously gates the potentials applied in the detect mode as shown in Fig. 2 and initiates sampling by the boxcar integrator.

At a fixed observing frequency, higher mass ions come into resonance at proportionately higher magnetic field strength. Thus from Eqs. (3) and (4) it follows that the integrated power absorption will be directly proportional to ion mass. Hence, to obtain true relative signal intensities, the detector output must be divided by ion mass.

The usefulness and accuracy of the method has been demonstrated by the satisfactory reproduction of rate constants in methyl chloride. A typical trace of intensity vs time for the positive ions observed in methyl chloride at 13.0 eV and 2.1×10^{-6} Torr[25] is shown in Fig. (4). The reaction sequence occurring in this system is[21,26–29]

$$CH_3Cl^+ + CH_3Cl \xrightarrow{k_1} CH_3ClH^+ + CH_2Cl, \quad (5)$$

$$CH_3ClH^+ + CH_3Cl \xrightarrow{k_2} CH_3ClCH_3^+ + HCl. \quad (6)$$

A solution to the kinetic equations for a simple primary (P), secondary (S), tertiary (T) ion system such as this yields the abundances of the various ions as

$$P = P(0)e^{-nk_1t}, \quad (7)$$

$$S = \frac{k_2P(0)}{k_2-k_1}(e^{-nk_1t} - e^{-nk_2t}), \quad (8)$$

$$T = \frac{k_1k_2P(0)}{k_2-k_1}\left(\frac{1-e^{-nk_1t}}{k_1} + \frac{e^{-nk_2t}-1}{k_2}\right), \quad (9)$$

where $P(0)$ represents the initial concentration of primary ions. A plot of $\log_{10}$(relative ion abundance) vs time for each of the ions in methyl chloride is shown in Fig. 5. The negative slope in Fig. 5 for the disappearance of CH_3Cl^+ gives $k_1 = 1.2\times10^{-9}$ cm^3·molecule^{-1}·sec^{-1}. This compares favorably with the values of 1.5×10^{-9} cm^3·molecule^{-1}·sec^{-1} obtained by Herod *et al.*,[28] 1.94×10^{-9} cm^3·molecule^{-1}·sec^{-1} obtained by McAskill,[27] and 1.25×10^{-9} cm^3·molecule^{-1}·sec^{-1} obtained by conventional ICR techniques.[29] The rate constant for formation of the dimethyl chloronium ion was obtained from the limiting negative slope in Fig. 5 for the disappearance of CH_3ClH^+. The value of $k_2 = 1.8\times10^{-10}$ cm^3·molecule^{-1}·sec^{-1} obtained agrees fairly well with the reported results of Herod *et al.*[28] (1.0×10^{-10} cm^3·molecule^{-1}·sec^{-1}) and of Beauchamp *et al.*[29] (1.4×10^{-10} cm^3·molecule^{-1}·sec^{-1}).

Ion losses are minimal. The data illustrated in Fig. 4 indicate a decrease in total ion abundance of ~3% after 100 msec. Storage of $>10^5$ ions in the same region leads to excessive losses which can be attributed to space charge effects. Space charge effects due to trapping of electrons with negative ions are particularly severe. This can be

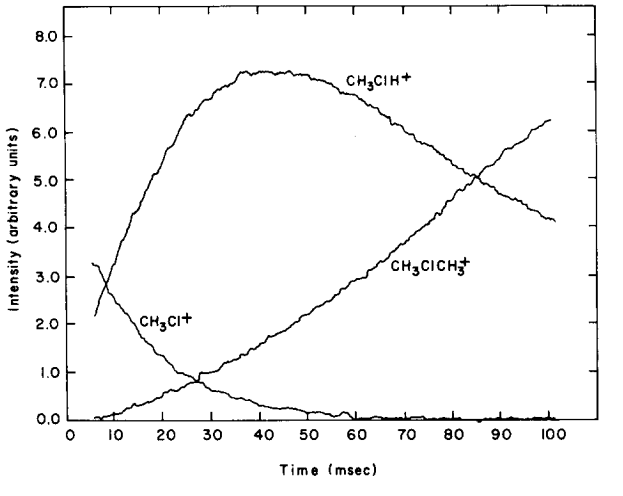

FIG. 4. Typical trace of variation of ion intensity with time for ions observed in methyl chloride at 13.0 eV and 2.1×10^{-6} Torr. Each trace represents a 5 min scan. The observing oscillator was operated at 307 kHz and the magnetic field was varied to observe each resonance.

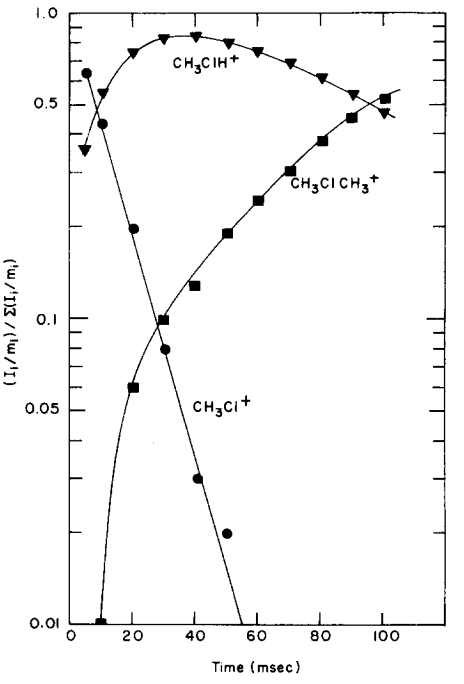

FIG. 5. Plot of $\log_{10}$(relative ion abundance) vs time for the three ions of the methyl chloride system.

avoided by ejecting electrons by excitation of their oscillatory motion in the trapping field.[15]

* Supported by the National Research Council of Canada (1970–present).
† Contribution No. 4379.

[1] A. A. Herod and A. G. Harrison, Int. J. Mass Spectrom. Ion Phys. **4**, 415 (1970), and references contained therein.
[2] R. A. Fluegge and D. Wobschall, Cornell Aeronautical Laboratory, U. S. Govt. Res. Develop. Rep. **69**, 63 (1969).
[3] R. T. McIver Jr., Rev. Sci. Instrum. **41**, 555 (1970).
[4] R. T. McIver Jr., and M. A. Haney, J. Amer. Chem. Soc. (to be published).
[5] M. A. Haney and R. T. McIver Jr., J. Amer. Chem. Soc. (to be published).
[6] R. T. McIver Jr. and R. C. Dunbar, Int. J. Mass Spectrom. Ion Phys. (to be published).
[7] S. E. Buttrill Jr., J. Chem. Phys. **50**, 4125 (1969).
[8] A. G. Marshall and S. E. Buttrill Jr., J. Chem. Phys. **52**, 2752 (1970).
[9] M. B. Comisarow, J. Chem. Phys. **55**, 205 (1971).
[10] J. L. Beauchamp, J. Chem. Phys. **46**, 1231 (1967).
[11] J. L. Beauchamp, Ann. Rev. Phys. Chem. **22** (1971).
[12] L. R. Anders, J. L. Beauchamp, R. C. Dunbar, and J. D. Baldeschwieler, J. Chem. Phys. **45**, 1062 (1966).
[13] J. L. Beauchamp and R. C. Dunbar, J. Amer. Chem. Soc. **92**, 1477 (1970).
[14] D. Holtz, J. L. Beauchamp, and J. R. Eyler, J. Amer. Chem. Soc. **92**, 7045 (1970).
[15] J. L. Beauchamp and J. T. Armstrong, Rev. Sci. Instrum. **40**, 123 (1969).
[16] L. R. Anders, J. Phys. Chem. **73**, 469 (1969).
[17] R. P. Clow and J. A. Futrell, Int. J. Mass Spectrom. Ion Phys. **4**, 165 (1970).
[18] W. T. Huntress Jr., M. M. Mosesman, and D. D. Elleman, J. Chem. Phys. **54**, 843 (1971).
[19] M. T. Bowers, D. D. Elleman, and J. L. Beauchamp, J. Phys. Chem. **72**, 3599 (1968).
[20] T. A. Lehman, T. A. Elwood, J. T. Bursey, and J. L. Beauchamp, J. Amer. Chem. Soc. **93**, 2108 (1971).
[21] J. D. Baldeschwieler, Science **159**, 263 (1968).
[22] For a detailed discussion of the motion of ions on equipotentials of the applied electrostatic fields, see T. B. McMahon and J. L. Beauchamp, Rev. Sci. Instrum. **42**, 1632 (1971).
[23] J. L. Beauchamp, Ph.D. thesis (Harvard University, 1967).
[24] J. D. Jackson, *Classical Electrodynamics* (Wiley, New York, 1962).
[25] Pressures were measured using a MKS Baratron by the procedure described in Ref. 14.
[26] S. K. Gupta, E. G. Jones, A. G. Harrison, and J. J. Myher, Can. J. Chem. **45**, 3107 (1967).
[27] N. A. McAskill, Aust. J. Chem. **22**, 2275 (1969).
[28] A. A. Herod, A. G. Harrison, and N. A. McAskill, Can. J. Chem. **49**, 2217 (1971).
[29] J. L. Beauchamp, D. Holtz, S. D. Woodgate, and S. L. Patt, J. Amer. Chem. Soc. (to be published).

THE REVIEW OF SCIENTIFIC INSTRUMENTS VOLUME 43, NUMBER 3 MARCH 1972

A Laser Velocimeter for Remote Wind Sensing*

T. R. LAWRENCE, D. J. WILSON, AND C. E. CRAVEN
Huntsville Research & Engineering Center, Lockheed Missiles & Space Company, Huntsville, Alabama 35807

I. P. JONES AND R. M. HUFFAKER
NASA–Marshall Space Flight Center, Huntsville, Alabama 35812

AND

J. A. L. THOMSON
Research Institute for Engineering Sciences, Wayne State University, Detroit, Michigan 48202

(Received 12 November 1971; and in final form, 13 December 1971)

A continuous wave carbon dioxide laser Doppler radar has been developed and applied to remote measurement of atmospheric wind velocity and turbulence. The carbon dioxide laser illuminates residual particulate matter in the atmosphere. Radiation scattered by these particles is homodyned with a local oscillator to provide the Doppler signal. The performance of the instrument is verified by comparison of wind velocity data recorded simultaneously by the laser Doppler system and a cup-anemometer–wind-vane system. Data were recorded, for 45 min intervals, of a single component of the horizontal wind velocity at an altitude of 10 m above the ground. The principle of the laser Doppler system and the theory of the system configuration are presented first, followed by the evaluation of the system. Sample data of a 20 min duration test run of a laser Doppler system are compared with conventional anemometer data. Further comparisons are given of the power spectral densities derived from the two time histories. All data comparisons indicate very close agreement of the two systems. Data inconsistencies are within the accuracy limitations of the conventional anemometer system. The range of the laser Doppler system during these tests was confined to approximately 30 m. Laser Doppler wind velocity data were observed at ranges exceeding 300 m; however, no conventional anemometer was set up at these ranges for data comparisons. Tests are planned for the near future, at which time comparison data at extended ranges will be recorded. These tests will also incorporate an on-line data processing system.

INTRODUCTION

When a beam of radiation is scattered or reflected by a target which is in motion relative to the source, the frequency of the scattered radiation differs from that of the incident by an amount dependent upon the target velocity, angle of scattering, and wavelength of the incident radiation. A measurement of this frequency change, the Doppler shift, can in turn be used to measure the velocity of the target. The advent of high power, highly monochromatic lasers has made possible the